

1 **Title:** Self-regulation of the brain's right frontal Beta rhythm using a brain-computer interface

2 **Short title:** Self-regulation of the right frontal Beta rhythm

3 **Author names:** Nadja Enz<sup>1</sup>, Jemima Schmidt<sup>1</sup>, Kate Nolan<sup>1</sup>, Matthew Mitchell<sup>1</sup>, Sandra  
4 Alvarez Gomez<sup>1</sup>, Miryam Alkayyali<sup>1</sup>, Pierce Cambay<sup>1</sup>, Magdalena Gippert<sup>1</sup>, Robert Whelan<sup>\*1,2</sup>,  
5 Kathy L. Ruddy<sup>\*1</sup>

6 **\*Equal contribution**

7 **Affiliations:** <sup>1</sup>School of Psychology and Institute of Neuroscience, Trinity College Dublin,  
8 Dublin, Ireland, <sup>2</sup>Global Brain Health Institute, Trinity College Dublin, Dublin, Ireland

9 **Corresponding Authors:**

10 Kathy L. Ruddy (ruddykl@tcd.ie), Lloyd Institute, Trinity College Institute of Neuroscience and  
11 School of Psychology, Trinity College Dublin, College Green, Dublin 2, Ireland  
12 Robert Whelan (robert.whelan@tcd.ie), Lloyd Institute, Trinity College Institute of  
13 Neuroscience and School of Psychology, Trinity College Dublin, College Green, Dublin 2,  
14 Ireland

15 **Acknowledgements:** The authors would like to thank Emma Wall, Aisling Martin and David  
16 M. Cole for assistance during data collection. Nadja Enz is supported by Irish Research  
17 Council postgraduate scholarship GOIPG/2018/537. Robert Whelan was supported by  
18 Science Foundation Ireland (16/ERC/3797); European Foundation for Alcohol Research  
19 (ERAB); Brain & Behavior Research Foundation (23599); Health Research Board HRAPOR-  
20 2015-1075. Kathy L. Ruddy would like to acknowledge funding from the Irish Research  
21 Council GOIPD/2017/798 and Health Research Board, Ireland HRB-EIA-2019-003.

22 **Competing interests:** The authors declare no competing financial or non-financial interests.

23 **Abstract**

24 Neural oscillations, or brain rhythms, fluctuate in a manner reflecting ongoing behavior.  
25 Whether these fluctuations are instrumental or epiphenomenal to the behavior remains  
26 elusive. Attempts to experimentally manipulate neural oscillations exogenously using non-  
27 invasive brain stimulation have shown some promise, but difficulty with tailoring stimulation  
28 parameters to individuals has hindered progress in this field. We demonstrate here using  
29 electroencephalography (EEG) neurofeedback in a brain-computer interface that human  
30 participants (n=44) learned over multiple sessions across a 6-day period to self-regulate their  
31 Beta rhythm (13-20 Hz) over the right inferior frontal cortex (rIFC). The modulation was evident  
32 only during neurofeedback task performance but did not lead to offline alteration of Beta  
33 rhythm characteristics at rest, nor to changes in subsequent cognitive behavior. Likewise, a  
34 control group (n=38) who underwent training of the Alpha rhythm (8-12 Hz) did not exhibit  
35 behavioral changes. Although the right frontal Beta rhythm has been repeatedly implicated as  
36 a key component of the brain's inhibitory control system, the present data suggest that its  
37 manipulation offline prior to cognitive task performance does not result in behavioral change.  
38 Thus, this form of neurofeedback training of the tonic Beta rhythm would not serve as a useful  
39 therapeutic target for disorders with dysfunctional inhibitory control as their basis.

40 **1 Introduction**

41 The synchronous firing of large populations of neurons across distributed brain networks  
42 produces rhythmic electric field fluctuations large enough to be detected at the scalp. The role  
43 – either causal or epiphenomenal – of the observed neural oscillations ('brain rhythms') for  
44 human behavior has been a topic of intense debate for decades. Traditionally, researchers  
45 have recorded neural oscillations from the scalp while participants perform cognitive tasks,  
46 thus investigating the correlation between brain signals and behavior. However, experimental  
47 manipulation is necessary in order to specify a causal role for neural oscillations (Herrmann  
48 et al., 2016; Vosskuhl et al., 2018).

49 Exogenous modulation of neural oscillations has previously been achieved using non-  
50 invasive brain stimulation techniques like transcranial alternating current stimulation (tACS,  
51 see Vosskuhl et al., 2018 for a review), oscillatory transcranial direct current stimulation  
52 (o-tDCS; e.g., Marshall et al., 2006), and repetitive transcranial magnetic stimulation (rTMS,  
53 e.g., Chung et al., 2015; Thut & Miniussi, 2009) (for reviews, see Dayan et al., 2013; Thut et  
54 al., 2011). These methods have generated mixed results with regards to effectiveness of  
55 neural modulation (for reviews, see Demirtas-Tatlidede et al., 2013; Enriquez-Geppert et al.,  
56 2013; Polanía et al., 2018; Thut et al., 2011) and impact upon cognitive behavior (Bestmann  
57 et al., 2015) with a key issue being heterogenous responses to the same stimulation across  
58 individuals (Adeyemo et al., 2012; Bergmann & Hartwigsen, 2020; Kasten et al., 2019).  
59 Individuals exhibit subtle idiosyncratic features of brain rhythms even within the commonly  
60 described bandwidths (Benwell et al., 2019; Haegens et al., 2014), however, methods like  
61 rTMS, tACS or o-tDCS typically target specific frequencies.

62 In addition to neuromodulation methods, brain-computer interface (BCI)-based  
63 neurofeedback can be used to endogenously train volitional modulation of brain signals. This  
64 approach enables participants to self-regulate brain rhythms which are intrinsic to the  
65 individual brain (Ros et al., 2010). Neurofeedback has been frequently tested and used as a  
66 therapeutic tool and studies have shown behavioral improvements in disorders such as

67 attention-deficit/hyperactivity disorder (ADHD; Jean Arthur Micoulaud-Franchi et al., 2014;  
68 Sonuga-Barke et al., 2013). However, to date there has been wide heterogeneity in research  
69 designs for neurofeedback protocols and it is difficult to draw conclusions regarding the  
70 effectiveness of neurofeedback to modify behavior (Omejc et al., 2019; Simon et al., 2021;  
71 Sitaram et al., 2017). As well as targeting individually tailored neural oscillation frequencies, it  
72 is important to target brain regions that are directly instrumental to the behavior under  
73 investigation. For example, electroencephalography (EEG)-neurofeedback from brain signals  
74 recorded over sensorimotor areas has shown some evidence of motor-skill improvement in  
75 healthy participants as well as clinical motor symptoms in ADHD or stroke patients (Jeunet et  
76 al., 2019). In addition, Hsueh et al. (2016) showed that neurofeedback of the frontoparietal  
77 Alpha rhythm improved working memory. Neurofeedback training of the Beta (13-20 Hz)  
78 rhythm in the past has predominantly targeted sensorimotor areas (e.g., Boulay et al., 2011;  
79 Vernon et al., 2003; Witte et al., 2013).

80 Inhibitory control is a core component of healthy executive function, and deficiencies  
81 with this aspect of cognition manifest in disorders such as ADHD (e.g., Lijffijt et al., 2005) or  
82 addiction (e.g., Luijten et al., 2011). Inhibitory control is believed to rely on fast and flexible  
83 command of the brain's Beta rhythm (Enz et al., 2021; Jana et al., 2020; Schaum et al., 2021;  
84 Swann et al., 2009; Wagner et al., 2017; Wessel, 2020), primarily in a pathway connecting  
85 right inferior frontal cortex (rIFC) and basal ganglia (Aron et al., 2014; Wessel & Aron, 2017).  
86 The Stop Signal Task (SST) measures this cognitive process (Logan & Cowan, 1984) by  
87 requiring the participant to cancel an already initiated motor response following an infrequent  
88 Stop cue. The Stop Signal Reaction Time (SSRT) is an estimation of the covert latency of the  
89 action cancellation process (Verbruggen et al., 2019).

90 In order to test whether selective self-regulation of specific brain rhythms could  
91 modulate specific cognitive processes, we designed a protocol whereby 82 participants  
92 learned over a 6-day period to either upregulate or downregulate the amplitude of their Beta  
93 or Alpha rhythm using direct neurofeedback in a BCI. We measured two distinct aspects of  
94 cognitive function; speed of proactive response inhibition (conditional SST [cSST]) and

95 working memory (2-Back Task). In a double-blinded mixed design with between-subject  
96 (neurofeedback types) and repeated measures (pre-post neurofeedback cognitive measures)  
97 factors, we tested the theory that causal manipulation of brain rhythms following  
98 neurofeedback training would have an observable impact upon behavior. Specifically, we  
99 hypothesized that learning to modulate the Beta rhythm over rIFC would impact positively  
100 upon speed of response inhibition, but not upon working memory. By contrast, we predicted  
101 that the control group undertaking Alpha neurofeedback would demonstrate no improvement  
102 in response inhibition.

103 **2 Method**

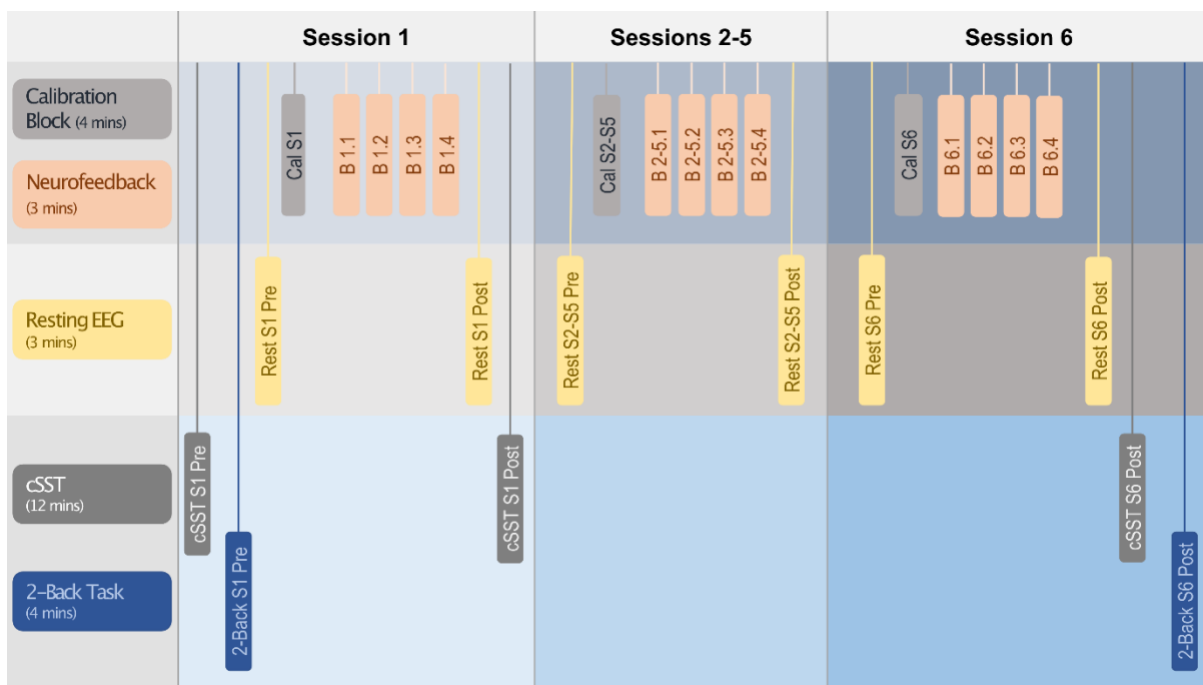
104 **2.1 Participants**

105 82 healthy adult human volunteers (age:  $24.27 \pm 7.74$  years [mean  $\pm$  SD]; 44 female; 69 right  
106 handed) participated in the study. Participants were reimbursed with either €5/hour and a  
107 completion bonus of €60 or with ECTS points. Inclusion criteria were: aged over 18, no history  
108 of traumatic brain injury and not currently experiencing any psychiatric disorder (self-reported).  
109 All participants provided written informed consent prior to participation. The experimental  
110 procedures were approved by the School of Psychology ethics committee of Trinity College  
111 Dublin and conducted in accordance with the Declaration of Helsinki.

112 **2.2 Study design**

113 Participants were allocated at random into four groups: '*Beta UP*' (n=26), '*Beta DOWN*' (n=18),  
114 '*Alpha UP*' (n=23) and '*Alpha DOWN*' (n=15). 'Beta' groups were trained to either increase  
115 ('UP') or decrease ('DOWN') their Beta (13-20 Hz) rhythm over the rIFC whereas 'Alpha'  
116 groups were trained to either increase ('UP') or decrease ('DOWN') their Alpha (8-12 Hz)  
117 rhythm over the same region. Each participant was trained over six sessions ('S1-6'). Where  
118 possible, sessions were scheduled for a similar time of the day.

119 The study design is illustrated in **Figure 1**. Each session consisted of one calibration  
120 ('*Cal S1-6*') and four neurofeedback training blocks ('*B1-6.1-4*') and each block lasted three  
121 minutes. Resting EEG was recorded in each session before ('*Rest S1-6 Pre*') and after ('*Rest*  
122 *S1-6 Post*') the four neurofeedback blocks. During S1 and S6, participants additionally  
123 performed two behavioral tasks, the cSST (experimental task) and the 2-Back Task (control  
124 task). The cSST was performed twice in S1, once before ('*cSST S1 Pre*') and once after  
125 ('*cSST S1 Post*') neurofeedback training whereas the 2-Back Task was only performed once  
126 ('*2-Back S1 Pre*'). In S6, both tasks were performed once after neurofeedback training ('*cSST*  
127 '*S6 Post*', '*2-Back S6 Post*'). For all sessions and tasks, the participants were seated  
128 comfortably in a chair in front of a computer screen in a soundproof, darkened room.



129 **Figure 1: Study design.** Behavioral tasks, baseline EEG measurements and neurofeedback training  
130 blocks are shown in sequential order for each of the six sessions. Each session was performed on a  
131 separate day. Abbreviations: cSST: conditional stop signal task.

### 132 **2.2.1 EEG recording**

133 During S1 and S6, 128-channel EEG data in the 10-5 system format were recorded using a  
134 128-channel BioSemi headcap connected to an ActiveTwo Biosemi system. During S2-S5,  
135 EEG was recorded from four active Ag/AgCl electrodes over the individual rIFC locus (see  
136 '*Functional rIFC localization*') with the same hardware. A reference electrode recorded data  
137 from Cz. For all sessions, three additional electrodes recorded the electrooculogram (right  
138 outer canthi for horizontal eye movements and ~2 cm below the left eye for vertical eye  
139 movements) as well as the right masseter muscle to detect facial movements.

### 140 **2.2.2 Resting EEG**

141 To record resting EEG, participants were instructed to fixate upon a black cross for 3 minutes  
142 with their eyes open and in a relaxed and stable body position.

143 **2.2.3 Conditional Stop Signal Task (cSST)**

144 The cSST was performed using Presentation® (Version 18.0, Neurobehavioral Systems, Inc.,  
145 Berkeley, CA, [www.neurobs.com](http://www.neurobs.com)) and EEG was recorded during the task. Each trial lasted  
146 1000 ms and was preceded by a fixation cross (1000 ms duration). During Go trials,  
147 participants were presented with black arrows pointing either to the right or left (Go signal; 750  
148 ms duration) and they were instructed to respond with their right or left index finger,  
149 respectively, as fast as possible via an Xbox 360 game controller. In one of four Go trials, the  
150 Go signal was followed by a black arrow pointing upwards (Stop signal; 250 ms duration) after  
151 a varying stop-signal delay (SSD). The participants were instructed to inhibit their button press  
152 on these Stop trials, but only if the Go signal was pointing in the critical direction. If a Stop  
153 signal appeared after a Go signal pointing in the non-critical direction, the participants were  
154 instructed to ignore the Stop signal and respond with a button press. The task was divided  
155 into four blocks; for the first two blocks the critical direction was right and for the last two blocks  
156 the critical direction was left. Each block consisted of 24 trials (18 Go trials and 6 Stop trials).  
157 The number of right and left pointing Go signals was equal in each block and presented in a  
158 randomized manner. The SSD was adjusted by a tracking algorithm, aiming to achieve a task  
159 difficulty resulting in 50% successful and 50% failed Stop trials. After a successful critical Stop  
160 trial (ignoring non-critical Stop trials), the SSD was increased, making the task harder and  
161 after a failed critical Stop trial (ignoring non-critical Stop trials), the SSD was decreased,  
162 making the task easier. The initial SSD was 250 ms and was subsequently adjusted using a  
163 double-limit algorithm (see Richards et al., 1999). The SSD could vary between 50 ms and  
164 450 ms. Following a Stop trial, the subsequent SSD value was chosen randomly between the  
165 current SSD and a pair of limits (higher or lower, as appropriate). These limits were designed  
166 to converge on the SSD that produced a 50% success rate and to be robust to fluctuations on  
167 individual trials. If a participant responded to the Go signal before Stop signal presentation,  
168 then the SSD was decreased for subsequent trials. All participants completed one block of  
169 fifteen practice trials where they received feedback before the real task.

170 **2.2.4 2-Back Task**

171 The 2-Back Task was programmed in Presentation® and no EEG was recorded. Participants  
172 were serially presented with randomized letters (500 ms duration each) with an interstimulus  
173 interval of 1000 ms. Participants were instructed to press the keyboard button number 1 if the  
174 current letter matched the letter presented 2 letters ago. Each block contained 10 targets (i.e.,  
175 matches) with the target frequency balanced across the block. The task consisted of two  
176 blocks and each block contained 50 letters.

177 **2.2.5 Functional rIFC localization**

178 After completion of the *cSST S1 Pre*, the raw EEG data recorded during the task was  
179 subjected to an immediate analysis in order to localize the rIFC region on the participant's  
180 topography. While scalp EEG cannot identify the source generator, studies using  
181 electrocorticography (Swann et al., 2009; Swann et al., 2012),  
182 magnetoencephalography/functional magnetic resonance imaging (fMRI; Schaum et al.,  
183 2020) and fMRI-guided repetitive transcranial magnetic stimulation (Sundby et al., 2021) have  
184 empirically demonstrated the link between right frontal scalp activity and rIFC. EEG data from  
185 the cSST were epoched into 2500 ms epochs with respect to the Go/Stop signal for Go trials  
186 and Stop trials, respectively. A short version of the Fully Automated Statistical Thresholding  
187 for EEG artefact Rejection plug-in (FASTER; Nolan et al., 2010;  
188 <https://sourceforge.net/projects/faster/>) was used to identify the most significant artefacts  
189 (e.g., eyeblinks and idiosyncratic muscle movements). EEG data were filtered at 13-20 Hz  
190 (Beta rhythm) and the amplitude was squared to obtain power estimates. Preprocessed EEG  
191 data were epoched into 100 ms to 300 ms after the Stop signal for successful and failed Stop  
192 trials. Additionally, a baseline (resting EEG data) was extracted from 1800 ms to 2000 ms  
193 after the Stop signal. These data were averaged over all trials for each channel and illustrated  
194 using topoplots. Four topoplots were shown; successful Stop trials, failed Stop trials,  
195 successful minus failed Stop trials and successful Stop trials minus baseline. The topoplots  
196 were then visually inspected and four right frontal electrodes showing the largest right frontal

197 power increase in the Beta range were identified as the individual participant's rIFC region.

198 This four-electrode cluster was used subsequently to provide signals for the neurofeedback.

199 **2.2.6 Calibration and neurofeedback blocks (B1-4)**

200 The OpenViBE Acquisition Server (OpenViBE, Renard et al., 2010, [www.openvibe.inria.fr](http://www.openvibe.inria.fr))  
201 received the EEG stream, and data were processed in real time using a custom OpenViBE  
202 Designer script. Data were processed using a 100-ms sliding window. First, the four individual  
203 rIFC channels as well as the reference channel (Cz) were selected. The selected data was  
204 then spatially (averaged over four rIFC channels) and temporally (13-20 Hz for 'Beta' groups,  
205 8-12 Hz for 'Alpha' groups) filtered. The data were then epoched into 100 ms windows and a  
206 power estimate of each 100 ms epoch was calculated by squaring the amplitude. Using  
207 LabStreamingLayer (<https://github.com/sccn/labstreaminglayer>), the resulting power  
208 estimates were then exported to MATLAB (R2017b, Mathworks, USA). Using a custom  
209 MATLAB script, the power estimates were visualized using the Psychophysics Toolbox  
210 (PsychToolbox; Brainard, 1997; <http://psychtoolbox.org>).

211 ***Calibration***

212 During the calibration block, the participants were instructed to first rest and fixate upon a red  
213 cross for 2 minutes and when the fixation cross turned green after 2 minutes, they were  
214 instructed to open and close their left hand for another 2 minutes. EEG was measured during  
215 the whole duration of the calibration block. This calibration procedure was performed in order  
216 to measure the participant's full power range of the respective frequency band (Beta or Alpha).  
217 The median power of the entire block was calculated.

218 ***Neurofeedback training (B1-4)***

219 During the four neurofeedback blocks, an avatar (bird for UP groups, fish for DOWN groups)  
220 was visualized on the screen and represented the participant's real-time power estimate  
221 output from OpenViBE. The avatar moved horizontally from left to right of the screen and either  
222 upwards or downwards depending on whether the power estimates increased or decreased,

223 respectively. The screen was separated horizontally by the median power from the calibration  
224 block into sky (above median) and sea (below median) (**Figure S2**). The top of the screen  
225 was equal to the maximum power of the calibration block and the bottom of the screen was  
226 equal to the minimum power of the calibration block. The UP groups were instructed to keep  
227 the bird in the sky (i.e., increase the power estimates) whereas the DOWN groups were  
228 instructed to keep the fish in the sea (i.e., decrease the power estimates). If the avatar deviated  
229 into the wrong environment (i.e., sky or sea), the environment turned red to give negative  
230 feedback and immediately turned back to normal when they returned into the desired zone.  
231 When participants were frequently reaching the top (UP groups) or bottom (DOWN groups) of  
232 the screen, the minimum and maximum limits were expanded by the X\*standard deviation of  
233 the power estimates of the calibration block. The game thus had 4 difficulty levels (X=0-4) and  
234 the level was increased if the participant was able to stay in the correct area (sky or sea) for  
235 more than 95% in a block. The participants were instructed to develop a mental strategy that  
236 does not involve movements, clenching teeth or tensing muscles. Participants were instructed  
237 to not close their eyes and to fixate upon the screen at all times.

### 238 **2.3 Data offline processing**

#### 239 **2.3.1 EEG offline preprocessing**

240 EEG data were digitized with a sampling rate of 512 Hz. EEG data preprocessing was carried  
241 out using the EEGLAB toolbox (Delorme and Makeig, 2004; <http://sccn.ucsd.edu/eeglab>) in  
242 conjunction with FASTER. The data were initially bandpass filtered between 1 Hz and 95 Hz,  
243 notch filtered at 50 Hz and average referenced across all scalp electrodes. Resting data and  
244 data from the calibration and neurofeedback blocks were subsequently epoched into windows  
245 of 1000 ms. Data from the cSST were epoched from 500 ms prior to Go/Stop signal onset to  
246 2000 ms after Go/Stop signal onset for Go trials and Stop trials, respectively. FASTER  
247 identified and removed artefactual (i.e., non-neural) independent components, removed  
248 epochs containing large artefacts (e.g., muscle twitches) and interpolated channels with poor  
249 signal quality. The remaining EEG data were then visually inspected by trained raters to

250 ensure good quality and that any remaining noisy data were removed. Specifically, trained  
251 raters identified any remaining artefacts in independent components (e.g., eyeblinks) and  
252 epochs containing idiosyncratic muscle/movement or transient electrode artifacts, and  
253 interpolated any channels that were noisy throughout all epochs of a participant. After  
254 preprocessing, EEG data were transformed using the current source density method (CSD;  
255 <https://psychophysiology.cpmc.columbia.edu/software/CSDtoolbox/index.html>; Kayser and  
256 Tenke, 2006) which is a reference-free montage to attenuate the effect of volume conduction  
257 in scalp EEG.

### 258 **2.3.2 Time-frequency transformation**

259 For all epochs, 2-dimensional representations of each electrode's time-frequency were  
260 estimated using a complex Morlet wavelet (range of logarithmically spaced 4-10 cycles for 39  
261 linearly spaced frequencies across 1-40 Hz). The squared magnitude of the convolved data  
262 was calculated to obtain power estimates. The power estimates were subsequently  
263 transformed to relative power. Power values of each given band from 1-28 Hz (Delta = 1-4 Hz,  
264 Theta = 5-7 Hz, Alpha = 8-12 Hz, Beta = 13-28 Hz) were expressed as a percentage of the  
265 total power within the spectrum (per channel and per given epoch). Beta bursts were extracted  
266 from non-relative time-frequency power estimates.

### 267 **2.3.3 Beta burst detection**

268 Beta burst detection was performed according to the method described in Enz et al. (2021).  
269 For each time-frequency power matrix, local maxima were detected using the MATLAB  
270 function *imregionalmax*. Beta bursts were then defined as local maxima that exceeded a  
271 defined threshold of 2x median power of the entire time-frequency matrix (across all trials per  
272 participant). Time-frequency matrices were then divided into ~25.39 ms time bins (also for  
273 analysis of relative power). The first and last time bins were removed from all trials due to an  
274 edge artefact that can occur when applying the MATLAB function *imregionalmax* (it detects  
275 artefactual local maxima on the edges of the time-frequency matrix). Beta burst rate (the sum

276 of the number of supra-threshold bursts) and Beta burst volume (the area under the curve of  
277 supra-threshold datapoints; see Enz et al., 2021) were then extracted per time bin. We also  
278 extracted the timing of the first Beta burst after the Stop/Go signal in the cSST EEG data.

279 **2.3.4 Selection of brain regions**

280 For the statistical analysis, EEG data were averaged over clusters of four electrodes from  
281 different regions of the brain. To interrogate EEG data from the rIFC, data were averaged over  
282 the four individually selected electrodes over the right frontal scalp area that were used during  
283 the neurofeedback training. Further, we also averaged clusters of four electrodes over the left  
284 motor cortex (D19/C3, D20, D12, D11), the right motor cortex (B22/C4, B23, B31, B30) and  
285 the occipital cortex (A23/Oz, A24, A28, A27) to test the specificity or generalization of effects  
286 beyond the trained region.

287 **2.4 Statistical analysis**

288 **2.4.1 Behavioral analysis**

289 Means and standard deviations were extracted for each participant for the following behavioral  
290 cSST measures: SSRT, intraindividual coefficient of variation (ICV), Go trial reaction time  
291 (RT), failed Stop trial RT, SSD, number of successful Stop trials, number of failed Stop trials,  
292 probability of successful stopping, probability of Go omissions, probability of choice errors.  
293 The SSRT was calculated using the integration method with replacement of Go omissions by  
294 the maximum RT (Verbruggen et al., 2019). All Go trials were included in the Go RT  
295 distribution, including Go trials with choice errors. Premature responses on failed Stop trials  
296 were included when calculating the probability of responding on a Stop trial and mean SSD.  
297 Participants with SSRT < 75 ms were excluded from all analyses. The ICV was calculated by  
298 dividing Go RT standard deviation by the mean Go RT.

299 For the 2-Back Task, the absolute number of target hits were calculated across both  
300 blocks (i.e., the maximum absolute number of target hits was 20).

301 **2.4.2 Neurofeedback training statistical analysis**

302 For resting EEG and for the calibration and neurofeedback blocks, data were averaged over  
303  $37 \times 25.39$  ms time bins. For the cSST,  $3 \times 25.39$  ms time bins were averaged to create  $\sim 75$   
304 ms time bins (6 time bins from -75 ms to 375 ms with respect to the Stop/Go signal). R (R  
305 Core Team, 2020) was used for all statistical analyses.

306 We first tested whether the neurofeedback training was effective. For this, we fit a  
307 linear mixed-effects model (LMM) using restricted maximum likelihood with relative Beta  
308 power over the rIFC as the outcome variable, with fixed effects of *Direction* (UP or DOWN)  
309 and *Timepoint* (Pre to Post neurofeedback training) and their two-way interaction, and with a  
310 random effect of *Participant*. We also calculated Cohen's D for each effect. The models were  
311 fit for the Beta and Alpha groups separately. We then also conducted the same analysis with  
312 relative Alpha power as outcome variable. We also looked at the same outcome variables  
313 from the other three brain regions (left motor cortex, right motor cortex, occipital cortex). This  
314 analysis was repeated with Beta burst rate and Beta burst volume as outcome variables. We  
315 ran a post-hoc test for significant interactions using the *emmeans* function in R. All post-hoc  
316 tests are Bonferroni corrected at  $0.05/2=0.025$ , correcting for the two directions (UP and  
317 DOWN).

318 Next, we looked at the effects of neurofeedback training on inhibitory control behavior.  
319 We again fit a LMM using restricted maximum likelihood with SSRT as the outcome variable,  
320 with fixed effects of *Direction* (UP or DOWN), *Timepoint* (Pre to Post neurofeedback training),  
321 *Rhythm* (Beta or Alpha) and their two- and three-way interactions, and with a random effect  
322 of *Participants*. We also calculated Cohen's D for each effect.

323 We then interrogated the relationship between the magnitude of the Pre-Post change  
324 in SSRT and the extent to which relative Beta power was modulated during neurofeedback  
325 training. For this we fit a linear model by robust regression using an M-estimator, with change  
326 in SSRT being the dependent variable and change in relative Beta power being the  
327 independent variable. We repeated this analysis with N-Back score, Go RT and ICV as  
328 outcome variables.

329 Next, we looked at the effects of neurofeedback training on resting EEG data collected  
330 before and after. We fit the same three-way LMM with relative Beta power, Beta burst rate  
331 and Beta burst volume over the rIFC as outcome variables.

332 Last, we looked at the effect of neurofeedback training on the brain activity while  
333 engaging inhibitory control behavior. Again, the same three-way LMM was fit for the time bins  
334 around the average SSRT with relative Beta power, Beta burst rate, Beta burst volume and  
335 timing of first Beta burst over the rIFC as outcome variables.

336 **2.5 Code and data accessibility**

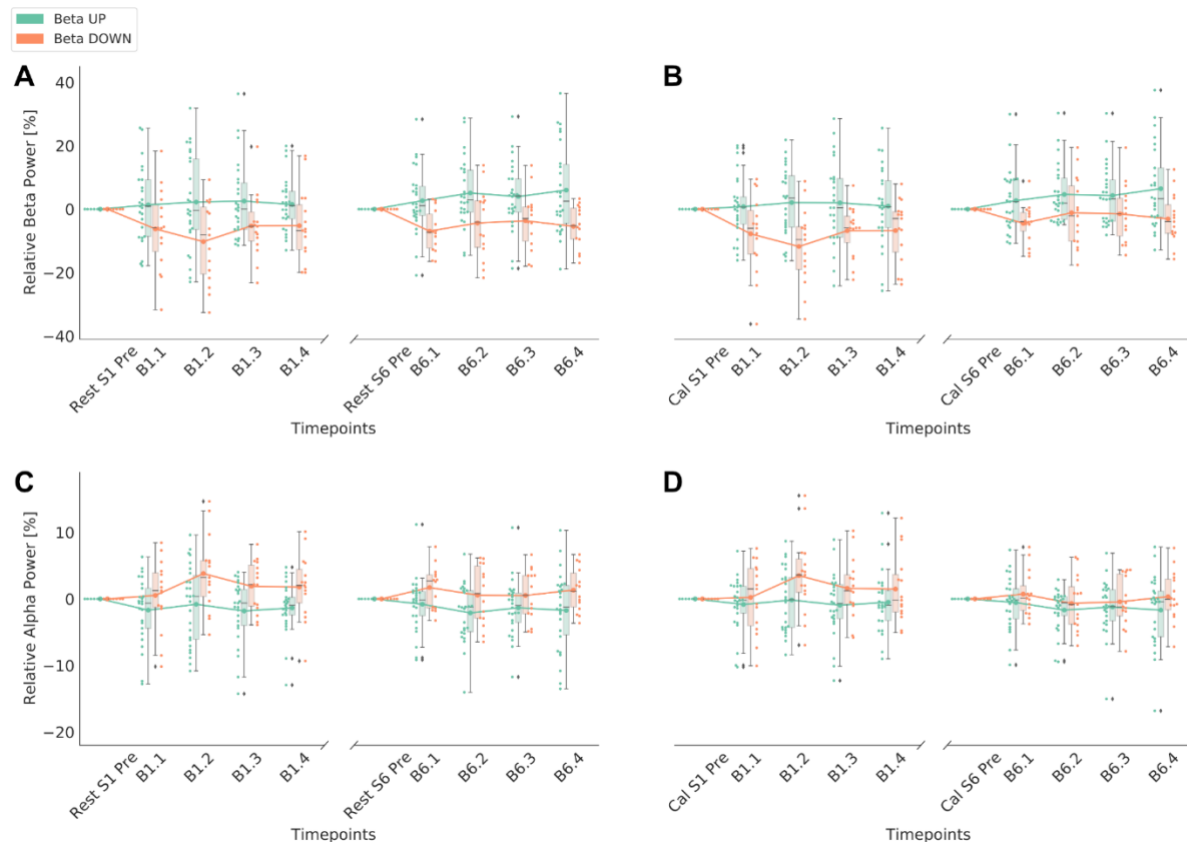
337 Custom written scripts and data summary files can be downloaded on the Open Science  
338 Framework at [URL to be inserted after acceptance].

339 **3 Results**

340 **3.1 Spectral power in the Beta band over rIFC was modulated by Beta neurofeedback**  
341 **training**

342 We first tested whether Beta and Alpha band spectral power was successfully modulated over  
343 rIFC by 6 days of neurofeedback in the trained directions (UP or DOWN), when quantified  
344 offline using optimal artefact rejection procedures. Linear mixed effects models were  
345 performed on EEG data recorded during BCI performance comparing spectral power at resting  
346 baseline on the first Day (Rest S1 Pre) to that at the end of the final (6<sup>th</sup>) Day (Block 6.4),  
347 within the two Beta subgroups. Beta power was significantly modulated from resting baseline  
348 on Day 1 to the final block of neurofeedback on Day 6, in a manner that differed depending  
349 on trained direction (**Figure 2A**). This was revealed by a Direction\*Timepoint interaction  
350 ( $F[1,40.04]=5.98$ ,  $p=0.019$ ,  $d=0.77$ ,  $n=44$ ). N.B.: All following post-hoc tests are Bonferroni  
351 corrected at  $0.05/2=0.025$  and all means are shown as estimated marginal means (EMM)  $\pm$   
352 standard error. Beta power modestly increased for the UP group (Pre  $62.0\pm3.03$  %, Post  
353  $64.2\pm3.03$  %; post-hoc test:  $t[39.1]=0.80$ ,  $p=0.43$ ) and significantly decreased for the DOWN  
354 group (Pre  $59.5\pm3.65$  %, Post  $50.5\pm3.89$  %; post-hoc test:  $t[41.5]=-2.47$ ,  $p=0.018$ ). The same  
355 pattern was evident when comparing data averaged within the calibration block performed  
356 immediately before training on Day 1 (Cal S1) to performance in the final block on Day 6  
357 ( $F[1,38.18]=13.99$ ,  $p=0.001$ ,  $d=1.21$ ,  $n=41$ ; **Figure 2B**). Beta power modestly increased for  
358 the UP group (Pre  $62.0\pm2.70$  %, Post  $64.2\pm2.67$  %; post-hoc test:  $t[38.5]=0.99$ ,  $p=0.33$ ) and  
359 significantly decreased for the DOWN group (Pre  $64.1\pm3.51$  %, Post  $52.3\pm3.51$  %; post-hoc  
360 test:  $t[38.0]=-3.96$ ,  $p=0.0003$ ). The calibration block data was used to establish the midline of  
361 the on-screen display in the neurofeedback game, which participants were required to keep  
362 an avatar above (UP) or below (DOWN). In this block, participants rested for two minutes,  
363 then conducted a left-hand finger tapping movement for two minutes in order to establish the  
364 full range of raw values associated with synchronization and desynchronization of the  
365 individual participant's Beta rhythm. **Figure 2A-B** show the time course of Beta power for S1

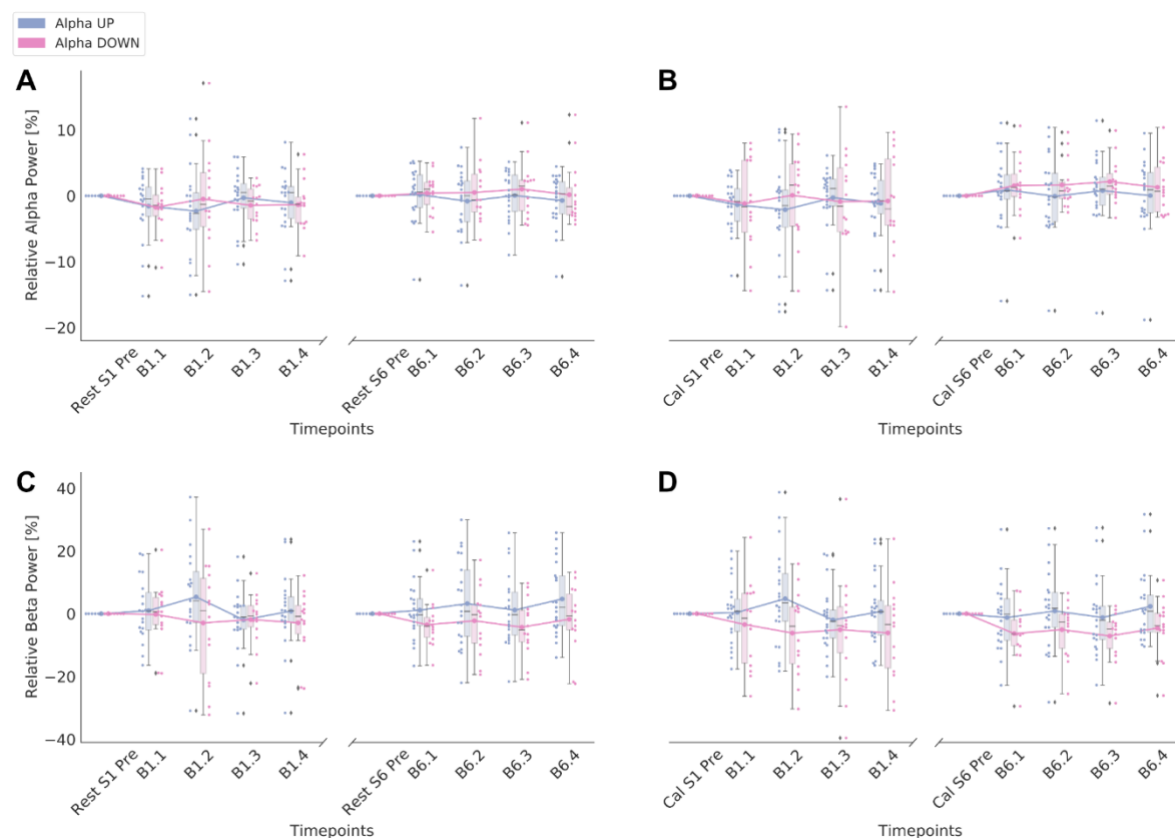
366 and S6 compared to resting baseline (**Figure 2A**) and calibration baseline (**Figure 2B**). See  
367 Supplementary Results 1 for acute within session modulation for Day 1 and Day 6.



368 **Figure 2: Neurofeedback training performance of Beta groups.** Performance of first and last session  
369 blocks is shown for Beta UP and Beta DOWN groups separately. Time course of relative power is  
370 corrected to the respective baseline. The boxplots show the medians and quartiles of the data, the  
371 whiskers extend to the rest of the distribution, except for points that are determined to be outliers. The  
372 swarm plots show individual datapoints and the line plots connect the means of each block. **A)** Relative  
373 Beta power is shown relative to the resting baseline before the first training block on Day 1. **B)** Relative  
374 Beta power is shown relative to the calibration baseline before the first training block on Day 1. **C)**  
375 Relative Alpha power is shown relative to the resting baseline before the first training block on Day 1.  
376 **D)** Relative Alpha power is shown relative to the calibration baseline before the first training block on  
377 Day 1.

378 Spectral power in the Beta band over rIFC was not significantly modulated from resting  
379 baseline during Alpha BCI training (Direction\*Timepoint interaction:  $F[1,31.94]=1.42$ ,  $p=0.24$ ,  
380  $d=0.42$ ,  $n=37$ ; **Figure 3C**). When comparing end of training (B6.4) to the calibration block on

381 Day 1, the Direction\*Timepoint interaction was significant ( $F[1,33.10]=4.38$ ,  $p=0.044$ ,  $d=0.73$ ,  
382  $n=36$ ) but post-hoc tests revealed that neither the UP nor DOWN groups showed significant  
383 modulation of the Beta rhythm from the calibration baseline (all  $p>0.13$ ; **Figure 3D**). Power in  
384 the Alpha band was similarly not modulated during Alpha neurofeedback (all  
385 Direction\*Timepoint interactions  $p>0.42$ ; **Figure 3A-B**), suggesting that training Alpha over  
386 rIFC was not achieved using this protocol.



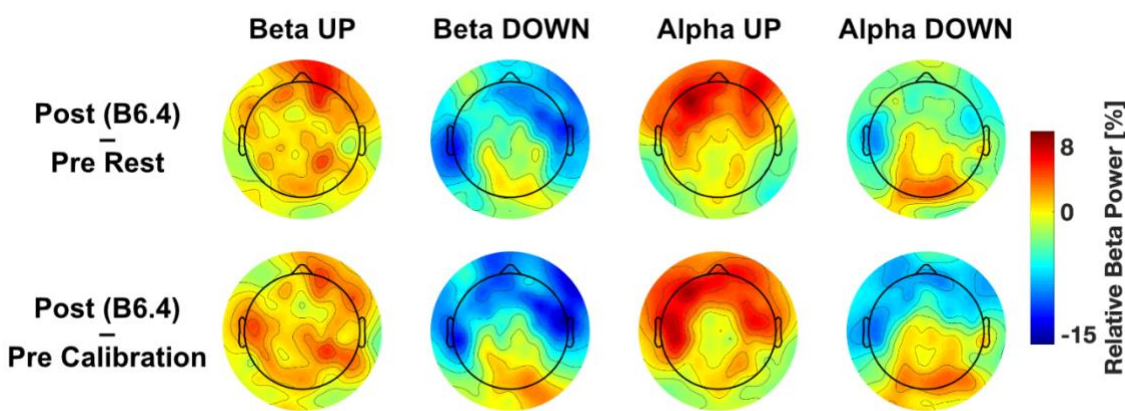
387 **Figure 3: Neurofeedback training performance of Alpha groups.** Performance of first and last  
388 session blocks is shown for Alpha UP and Alpha DOWN groups separately. Time course of relative  
389 power is corrected to the respective baseline. The boxplots show the medians and quartiles of the data,  
390 the whiskers extend to the rest of the distribution, except for points that are determined to be outliers.  
391 The swarm plots show individual datapoints and the line plots connect the means of each block. **A)**  
392 Relative Alpha power is shown relative to the resting baseline before the first training block on Day 1.  
**B)** Relative Alpha power is shown relative to the calibration baseline before the first training block on  
393 Day 1. **C)** Relative Beta power is shown relative to the resting baseline before the first training block  
394 on Day 1. **D)** Relative Beta power is shown relative to the calibration baseline before the first training  
395 block on Day 1.

397 **3.2 Cross frequency effects and modulation of neural oscillations beyond rIFC**

398 We first investigated whether power in the Alpha band was modulated during neurofeedback  
399 targeting the Beta rhythm (**Figure 2C-D**). When comparing calibration baseline Alpha power  
400 on Day 1 to Alpha power during neurofeedback attempting to regulate Beta, significant  
401 modulation was detected at the end of Day 6 ( $F[1,38.33]=4.78$ ,  $p=0.035$ ,  $d=-0.71$ ,  $n=41$ ).  
402 Alpha power modestly decreased for the UP group (Pre  $16.1\pm1.26\%$ , Post  $15.8\pm1.24\%$ ; post-  
403 hoc test:  $t[38.5]=-0.21$ ,  $p=0.83$ ) and significantly increased for the DOWN group (Pre  
404  $17.0\pm1.64\%$ , Post  $20.5\pm1.64\%$ ; post-hoc test:  $t[38.0]=2.60$ ,  $p=0.013$ ). It is notable however  
405 that although this demonstrates that Alpha was modulated during training based upon  
406 neurofeedback of the Beta rhythm, the direction of change was opposite (Alpha decreased in  
407 the Beta UP training and vice versa). Also, the absolute effect sizes for Alpha modulation  
408 during Beta training range from 0.23-0.71, whereas Beta modulation absolute effect sizes  
409 were substantially larger (0.61-1.21). On the final Day of training, Alpha power was not  
410 modulated acutely (i.e., within session) during Beta training when comparing power during the  
411 final neurofeedback block to the resting baseline on the same day ( $F[1,38.75]=3.16$ ,  $p=0.08$ ,  
412  $d=-0.57$ ,  $n=41$ ), nor to the calibration block ( $F[1,37.06]=1.35$ ,  $p=0.25$ ,  $d=-0.38$ ,  $n=41$ ). Thus,  
413 the effects of Beta training were largely selective to the Beta rhythm.

414 To investigate effects spanning beyond the trained cluster of electrodes over rIFC, we  
415 tested whether Beta Power at three other scalp sites was modulated during neurofeedback of  
416 Beta signals recorded from rIFC. We chose clusters of four electrodes over right and left motor  
417 cortex and occipital cortex for comparison and performed mixed effects models testing for  
418 Direction\*Timepoint interactions, as before. No significant interactions in any of the three  
419 regions were detected when comparing resting baseline Beta power to Beta power during the  
420 final neurofeedback block on Day 6 (all  $p>0.12$ ). However, when comparing Beta power from  
421 the initial calibration block on Day 1 to power during the final block on Day 6, significant  
422 Direction\*Timepoint interactions were revealed for both right ( $F[1,38.45]=8.46$ ,  $p=0.006$ ,  
423  $d=0.94$ ,  $n=41$ ) and left ( $F[1,38.36]=6.58$ ,  $p=0.014$ ,  $d=0.83$ ,  $n=41$ ) motor regions, but no  
424 modulation was evident in the occipital region ( $F[1,35.03]=0.29$ ,  $p=0.59$ ,  $d=-0.18$ ,  $n=41$ ). For

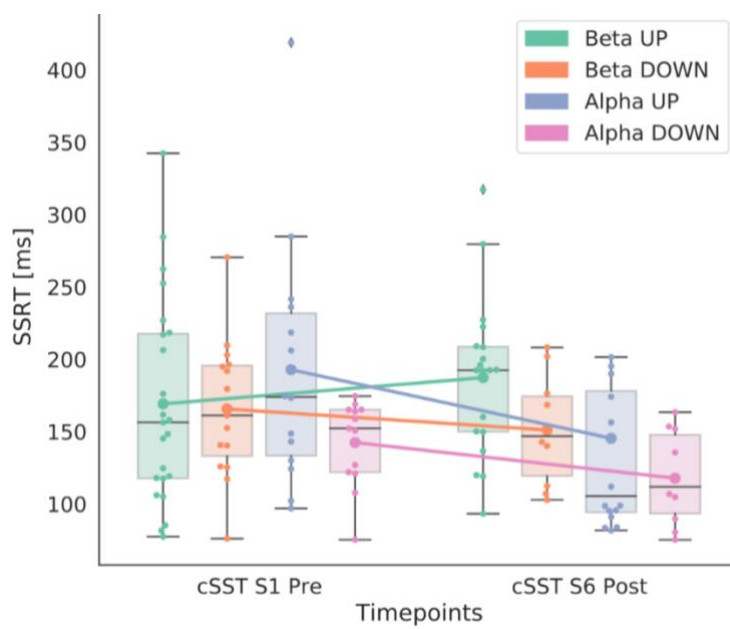
425 the right motor region, Beta power modestly increased for the UP group (Pre  $56.9 \pm 2.34\%$ ,  
426 Post  $58.9 \pm 2.31\%$ ; post-hoc test:  $t[38.5] = 0.92$ ,  $p = 0.36$ ) and significantly decreased for the  
427 DOWN group (Pre  $59.4 \pm 3.04\%$ , Post  $51.3 \pm 3.04\%$ ; post-hoc test:  $t[38.0] = -2.96$ ,  $p = 0.005$ ).  
428 For the left motor region, Beta power modestly increased for the UP group (Pre  $57.6 \pm 2.29\%$ ,  
429 Post  $59.5 \pm 2.27\%$ ; post-hoc test:  $t[38.4] = 1.13$ ,  $p = 0.26$ ) and significantly decreased for the  
430 DOWN group (Pre  $57.4 \pm 2.99\%$ , Post  $52.3 \pm 2.99\%$ ; post-hoc test:  $t[38.0] = -2.37$ ,  $p = 0.023$ ).  
431 Topoplots for post-training minus pre-training are shown for each training group for both Beta  
432 power (**Figure 4**) and Alpha power (**Figure S1**).



433 **Figure 4: Change in Beta power pre- to post-neurofeedback training.** Topoplots show relative Beta  
434 power for the last block of neurofeedback training (Post B6.4) minus resting EEG before first block of  
435 neurofeedback training (Pre Rest) as well as for the last block of neurofeedback training (Post B6.4)  
436 minus calibration block (Pre Calibration). Topoplots are shown separately for each group (Beta UP,  
437 Beta DOWN, Alpha UP, Alpha DOWN).

438 **3.3 Change in inhibitory control behavior modulated by neurofeedback training**

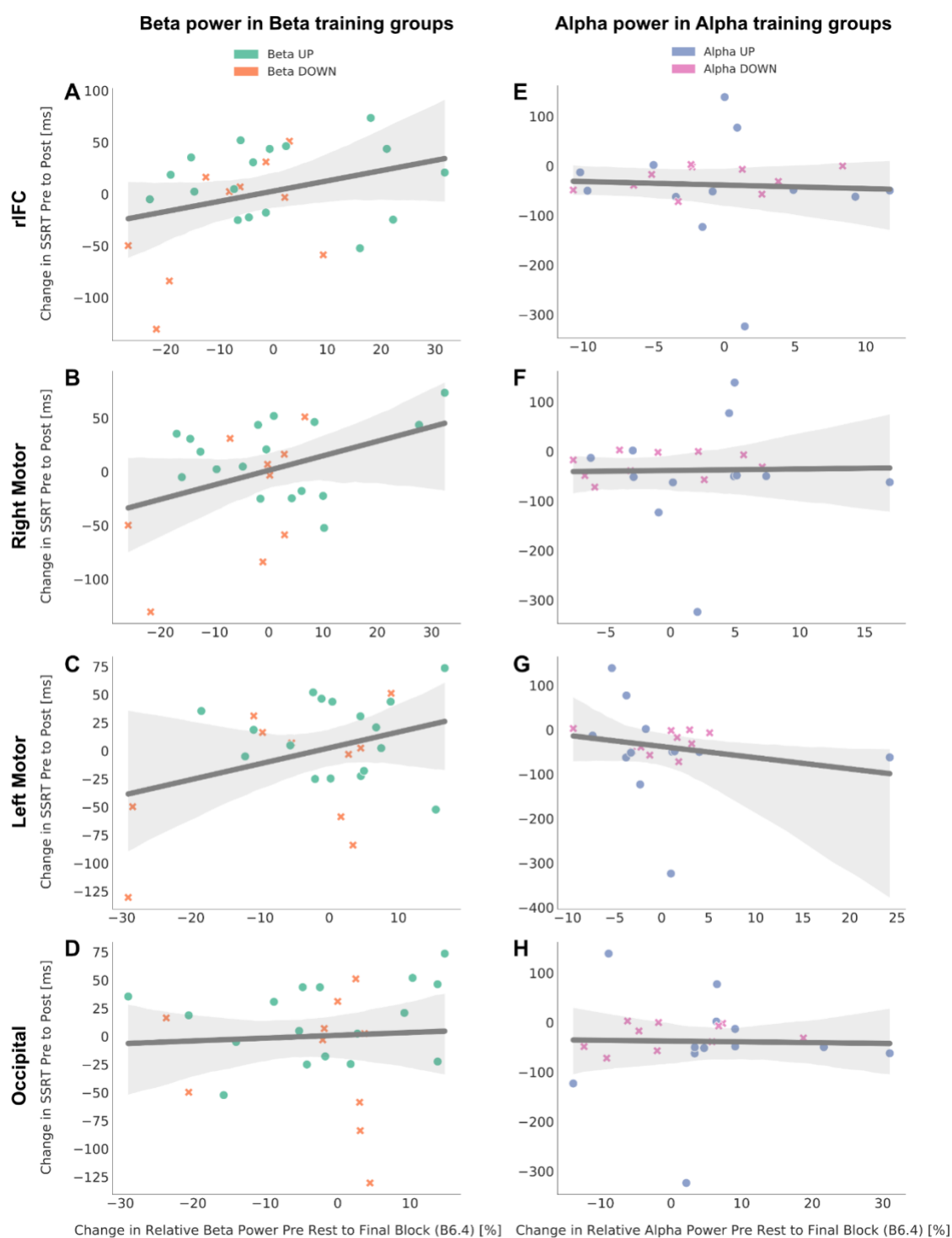
439 Behavioral data of the cSST are displayed in **Table S1**. To assess whether neurofeedback  
440 training had any effect upon inhibitory control behavior in the cSST (i.e., upon SSRT, the  
441 speed of inhibitory control), we performed a mixed effects model with three fixed effects;  
442 Rhythm (Alpha or Beta), Direction (UP or DOWN) and Timepoint (pre or post training). There  
443 was no 3-way Rhythm\*Direction\*Timepoint interaction ( $F[1,54.88]=2.32$ ,  $p=0.13$ ,  $d=0.41$ ,  
444  $n=71$ ). There was a fixed effect of Timepoint ( $F[1,54.88]=4.35$ ,  $p=0.042$ ,  $d=0.28$ ,  $n=71$ ),  
445 revealing that SSRTs generally improved over time regardless of BCI training type (EMMs  
446 averaged over levels of Rhythm and Direction: Pre  $166\pm7.86$  ms, Post  $147\pm8.54$  ms). **Figure**  
447 **5** shows the mean pre and post SSRTs for each group.



448 **Figure 5: SSRTs of each training group.** The SSRTs are shown for each training group for pre (Day  
449 1) and post (Day 6) neurofeedback training. The boxplots show the median and quartiles of the data,  
450 the whiskers extend to the rest of the distribution, except for points that are determined to be outliers.  
451 The swarm plots show individual datapoints and the line plots connect the means of each block.  
452 Abbreviations: SSRT: Stop signal reaction time; cSST: conditional stop signal task.

453 To investigate whether each individual's pre-post change in SSRT could be predicted  
454 by the extent to which their Beta rhythm was modulated, we performed Robust Regression  
455 analyses with change in SSRT as outcome variable and change in Beta rhythm (resting  
456 baseline from Day 1 to final block on Day 6) as predictor. The extent of change in the Beta  
457 rhythm as a result of training did not significantly predict improvement in SSRT from Pre-Post  
458 (slope=0.81, df=25, F=2.06, p=0.16, n=22; **Figure 6A**). The same was evident when tested at  
459 the right motor electrode cluster (slope=1.15, df=25, F=2.76, p=0.11, n=22; **Figure 6B**), left  
460 motor cluster (slope=1.22, df=25, F=2.38, p=0.14, n=22; **Figure 6C**), and occipital cluster  
461 (slope=0.46, df=25, F=0.41, p=0.53, n=22; **Figure 6D**). Training related change in Alpha  
462 power for those training Alpha rhythms was not predictive of behavioral change in SSRT (all  
463 p>0.26; **Figure 6E-H**).

464 We additionally tested whether neurofeedback training impacted other aspects of  
465 cognitive function, including working memory (2-Back Task), processing speed (Go RT; Go  
466 reaction times in the cSST) and performance variability (ICV; intra-coefficient of variation in  
467 the cSST). No 3-way interactions emerged between Rhythm\*Direction\*Timepoint (all p>0.41),  
468 but for Go RT there was a significant 2-way Rhythm\*Timepoint interaction ( $F[1,75.34]=4.82$ ,  
469 p=0.031, d=0.47, n=82). Post-hoc tests are indicating a general improvement in speed  
470 predominantly in the Beta group, revealing that Go RT significantly decreased for the Beta  
471 group (Pre 484±7.07 ms, Post 463±7.31 ms; post-hoc test:  $t[5.40]=3.44$ , p=0.001) but did not  
472 significantly decrease for the Alpha group (Pre 480±7.65 ms, Post 478±7.79 ms; post-hoc test:  
473  $t[74.4]=0.24$ , p=0.82).



474 **Figure 6: Association between change in SSRT and change in relative power.** Each plot shows the  
475 linear regression fit line of the data in dark grey as well as the confidence interval in light grey. Please  
476 note the difference in scale across all plots. The associations are shown for an average of four electrodes  
477 in four different brain regions (rIFC, right motor, left motor, occipital). **A-D)** show the association  
478 between change in SSRT and change in relative Beta power in the Beta groups (UP and DOWN). **E-H)**  
479 show the association between change in SSRT and change in relative Alpha power in the Alpha  
480 groups (UP and DOWN). Abbreviations: SSRT: stop signal reaction time; rIFC: right inferior frontal  
481 cortex.

482 **3.4 Resting spectral Beta power was not altered by neurofeedback training**

483 Comparing resting EEG data from before training (Rest S1 Pre), after Day 1 of training (Rest  
484 S1 Post) and Post training on Day 6 (Rest S6 Post), mixed effects models revealed no  
485 significant Direction\*Timepoint interactions for the Beta group ( $F[2,79.42]=0.34$ ,  $p=0.71$ ,  
486  $n=44$ ), suggesting that training related modulations of Beta power were only evident when  
487 engaged in the task but did not lead to a lasting change in the background (resting) tonic Beta  
488 level.

489 **3.5 Modulation of Beta burst characteristics by training the tonic Beta Rhythm**

490 We investigated whether training to modulate tonic Beta Power over rIFC has consequences  
491 for Beta burst characteristics. Beta burst rate was not altered during or after training at any of  
492 the timepoints tested (all  $p>0.277$ ). Burst volume was significantly modulated at the end of the  
493 first Day of training when comparing burst volume in the last block of Day 1 to that detected in  
494 the calibration block on the same Day (Direction\*Timepoint interaction:  $F[1,37.48]=6.14$ ,  
495  $p=0.02$ ,  $d=0.81$ ,  $n=40$ ). Burst volume significantly increased for the UP group (Pre  $5962\pm1744$   
496 a.u., Post  $9769\pm1771$  a.u.; post-hoc test:  $t[36.6]=2.20$ ,  $p=0.03$ ) and modestly decreased for  
497 the DOWN group (Pre  $8560\pm2311$  a.u., Post  $5336\pm2251$  a.u.; post-hoc test:  $t[37.0]=-1.43$ ,  
498  $p=0.16$ ).

499 **3.6 Brain activity while performing the cSST was not modified following training**

500 There were no significant differences in neural activity (Beta power, burst rate, burst volume,  
501 timing of first burst) recorded during cSST performance at the start of the first day of training  
502 compared to the end of Day 6 of training (all  $p>0.40$ ).

503 **4 Discussion**

504 We have demonstrated here that using neurofeedback in a BCI it is possible to train human  
505 participants to self-regulate their Beta rhythm over the rIFC, but that this has no observable  
506 consequences upon subsequent inhibitory control behavior. Participants trained over a 6-day  
507 period to upregulate or downregulate the amplitude of their Beta rhythm over rIFC, resulting  
508 in the predicted directional changes to Beta power. Concomitant changes at other (untrained)  
509 scalp regions and other frequency bands were of lower magnitude, indicating good specificity  
510 of the neurofeedback protocol for modulating the trained rhythm, direction and region. The  
511 extent to which each individual's SSRT changed pre-post training was however, not predicted  
512 by the magnitude of their training-related change in Beta over rIFC. This was also not the case  
513 for the control group undergoing Alpha training. Although the right frontal Beta rhythm has  
514 been repeatedly implicated as a key component of the brain's inhibitory control system, the  
515 present data suggest that improving the ability to self-regulate the rhythm does not result in  
516 behavioral change in an inhibitory control task.

517 Training related modulation of the Beta rhythm was only manifest during the  
518 neurofeedback task and did not alter EEG signals measured subsequently at rest or during  
519 cSST task performance. The current experimental design did not permit us to investigate  
520 whether online (i.e., during cSST task performance) self-regulation of the Beta rhythm would  
521 impact upon behavior, although this may be an interesting future extension of the work.  
522 Additionally, in the BCI task, neurofeedback was provided on the amplitude of the tonic  
523 (background) Beta rhythm. Further analyses revealed that this style of regulation of tonic Beta  
524 power had no impact on the rate or volume of transient burst-like high amplitude events in the  
525 Beta frequency range. This adds weight to the emerging view that so called 'Beta bursts' are  
526 a phenomena distinct from the ongoing background or 'tonic' oscillation at the same frequency  
527 (Bonaiuto et al., 2021; Little et al., 2019). Timing and magnitude of Beta bursts critically impact  
528 upon subsequent motor performance (Little et al., 2019) and whether attempts to inhibit a  
529 response are successful or not (Enz et al., 2021; Wessel, 2020). Although participants learned

530 to modulate the amplitude of their Beta rhythm over rIFC, this gradual, tonic background  
531 change in Beta during the distinct 3-minute neurofeedback blocks had no impact upon  
532 subsequent inhibitory control behavior. In order to modify Beta bursts using the BCI, it may be  
533 necessary to provide feedback specifically tailored to detect and influence bursting in real-  
534 time (online), rather than simply of generalized (and offline) regulation of tonic Beta (e.g., He,  
535 2020).

536 In the protocol used in the current study, neurofeedback targeting downregulation of  
537 Beta oscillations was more impactful than upregulation. It is likely that downregulation is simply  
538 easier for participants to perform, as it is known that engaging a brain region in a mental  
539 process (such as motor imagery), tends to lead Beta (and Alpha) to desynchronize in the  
540 region (Jensen & Mazaheri, 2010). Over the 6-day training period, participants learned to tailor  
541 their mental imagery strategies to optimally engage rIFC in order to achieve tangible real-time  
542 control over the movement of the avatar on screen. Our results leave open the possibility that  
543 it may be the ability to flexibly engage (and remove) Beta oscillations in the form of precisely  
544 timed bursts that predicts behavioral performance, rather than the tonic level per se.

545 While the neurofeedback training we employed was effective for regulating the Beta  
546 rhythm over rIFC, Alpha modulation at this scalp location was not achieved. The lack of Alpha  
547 modulation over rIFC may be due to the fact that Beta is the predominant resonating frequency  
548 in this location, and has been repeatedly implicated in the functioning of this region (Schaum  
549 et al., 2021; Sundby et al., 2021; Swann et al., 2009; Swann et al., 2012; Wagner et al., 2017).  
550 Further, for all participants (even those in the Alpha group) we performed the same functional  
551 localizer to detect the precise cluster of electrodes corresponding to the right frontal scalp  
552 location showing most substantial Beta synchronization during the cSST. This cluster of  
553 electrodes, selected for exhibiting strong Beta activity during inhibitory control, was used to  
554 tailor the BCI neurofeedback for both Alpha and Beta groups. Optimizing the BCI for Beta  
555 using this method may further explain why Alpha modulation was not achieved at the rIFC  
556 site.

557 Previous studies using implanted electrodes have reported that positive effects upon  
558 motor behavior could be achieved in macaques (Khanna & Carmena, 2017) and humans with  
559 Parkinson's disease (Bichsel et al., 2021) using BCI to train self-regulation of the brain's Beta  
560 rhythm. Here we build upon and extend these initial findings by making the advance to non-  
561 invasive scalp recorded EEG signals in humans, demonstrating that volitional modulation of  
562 Beta oscillations was achieved within 6 days of training. The BCI neurofeedback protocol  
563 demonstrated good spatial and temporal specificity, modulating primarily the targeted region,  
564 rhythm and direction. The lack of behavioral consequences further adds weight to the  
565 emerging picture in recent research showing that the right frontal Beta signature associated  
566 with stopping may not exert a direct functional influence upon the behavior. Indeed, Errington  
567 et al. (2020) demonstrated using depth electrodes in macaques that while Beta bursts were  
568 associated with inhibitory control, successful stopping could occur even on trials where no  
569 bursts were detected. They also highlighted that the occurrence of Beta bursts during Stop  
570 trials was generally very low (~15% of trials), and as such may only represent one component  
571 of a more complex neural mechanism underlying inhibitory control.

572 Using non-invasive BCI technology, volitional and causal self-regulation was  
573 achieved without the need for exogenous stimulation, paving the way for easier real-world  
574 application of neuromodulation to alter brain rhythms experimentally. The present data  
575 suggest, however, that offline neurofeedback training of the tonic Beta rhythm may not serve  
576 as a useful therapeutic target for disorders with dysfunctional inhibitory control as their basis.

577 **References**

578 Adeyemo, B. O., Simis, M., Macea, D. D., & Fregni, F. (2012). Systematic review of  
579 parameters of stimulation, clinical trial design characteristics, and motor outcomes in  
580 non-invasive brain stimulation in stroke. *Frontiers in Psychiatry*, 3(November), 1–27.  
581 <https://doi.org/10.3389/fpsyg.2012.00088>

582 Aron, A. R., Robbins, T. W., & Poldrack, R. A. (2014). Inhibition and the right inferior frontal  
583 cortex: One decade on. *Trends in Cognitive Sciences*, 18(4), 177–185.  
584 <https://doi.org/10.1016/j.tics.2013.12.003>

585 Benwell, C. S. Y., London, R. E., Tagliabue, C. F., Veniero, D., Gross, J., Keitel, C., & Thut,  
586 G. (2019). Frequency and power of human alpha oscillations drift systematically with  
587 time-on-task. *NeuroImage*, 192, 101–114.  
588 <https://doi.org/10.1016/j.neuroimage.2019.02.067>

589 Bergmann, T. O., & Hartwigsen, G. (2020). Inferring causality from noninvasive brain  
590 stimulation in cognitive neuroscience. *Journal of Cognitive Neuroscience*, 33(2), 195–  
591 225. [https://doi.org/10.1162/jocn\\_a\\_01591](https://doi.org/10.1162/jocn_a_01591)

592 Bestmann, S., de Berker, A. O., & Bonaiuto, J. (2015). Understanding the behavioural  
593 consequences of noninvasive brain stimulation. *Trends in Cognitive Sciences*, 19(1),  
594 13–20. <https://doi.org/10.1016/j.tics.2014.10.003>

595 Bichsel, O., Stieglitz, L. H., Oertel, M. F., Baumann, C. R., Gassert, R., & Imbach, L. L.  
596 (2021). Deep brain electrical neurofeedback allows Parkinson patients to control  
597 pathological oscillations and quicken movements. *Scientific Reports*, 11, 7973.  
598 <https://doi.org/10.1038/s41598-021-87031-2>

599 Bonaiuto, J. J., Little, S., Neymotin, S. A., Jones, S. R., Barnes, G. R., & Bestmann, S.  
600 (2021). Laminar dynamics of beta bursts in human motor cortex. *BioRxiv*, 431412.  
601 Retrieved from <https://doi.org/10.1101/2021.02.16.431412>

602 Boulay, C. B., Sarnacki, W. A., Wolpaw, J. R., & McFarland, D. J. (2011). Trained  
603 modulation of sensorimotor rhythms can affect reaction time. *Clinical Neurophysiology*,

604 122(9), 1820–1826. <https://doi.org/10.1016/j.clinph.2011.02.016>

605 Brainard, D. H. (1997). The Psychophysics Toolbox. *Spatial Vision*, 10, 433–436.

606 <https://doi.org/10.1163/156856897X00357>

607 Chung, S. W., Rogasch, N. C., Hoy, K. E., & Fitzgerald, P. B. (2015). Measuring brain

608 stimulation induced changes in cortical properties using TMS-EEG. *Brain Stimulation*,

609 8(6), 1010–1020. <https://doi.org/10.1016/j.brs.2015.07.029>

610 Dayan, E., Censor, N., Buch, E. R., Sandrini, M., & Cohen, L. G. (2013). Noninvasive brain

611 stimulation: From physiology to network dynamics and back. *Nature Neuroscience*,

612 16(7), 838–844. <https://doi.org/10.1038/nn.3422>

613 Delorme, A., & Makeig, S. (2004). EEGLAB: An open source toolbox for analysis of single-

614 trial EEG dynamics including independent component analysis. *Journal of*

615 *Neuroscience Methods*, 134(1), 9–21. <https://doi.org/10.1016/j.jneumeth.2003.10.009>

616 Demirtas-Tatlidede, A., Vahabzadeh-Hagh, A. M., & Pascual-Leone, A. (2013). Can

617 noninvasive brain stimulation enhance cognition in neuropsychiatric disorders?

618 *Neuropharmacology*, 64, 566–578. <https://doi.org/10.1016/j.neuropharm.2012.06.020>

619 Enriquez-Geppert, S., Huster, R. J., & Herrmann, C. S. (2013). Boosting brain functions:

620 Improving executive functions with behavioral training, neurostimulation, and

621 neurofeedback. *International Journal of Psychophysiology*, 88(1), 1–16.

622 <https://doi.org/10.1016/j.ijpsycho.2013.02.001>

623 Enz, N., Ruddy, K. L., Rueda-Delgado, L. M., & Whelan, R. (2021). Volume of  $\beta$ -Bursts, But

624 Not Their Rate, Predicts Successful Response Inhibition. *The Journal of Neuroscience*,

625 41(23), 5069–5079. <https://doi.org/10.1523/jneurosci.2231-20.2021>

626 Errington, S. P., Woodman, G. F., & Schall, J. D. (2020). Dissociation of Medial Frontal  $\beta$ -

627 Bursts and Executive Control. *Journal of Neuroscience*, 40(48), 9272–9282.

628 <https://doi.org/10.1017/CBO9781107415324.004>

629 Haegens, S., Cousijn, H., Wallis, G., Harrison, P. J., & Nobre, A. C. (2014). Inter- and intra-

630 individual variability in alpha peak frequency. *NeuroImage*, 92, 46–55.

631 <https://doi.org/10.1016/j.neuroimage.2014.01.049>

632 He, S. (2020). Neurofeedback-linked suppression of cortical beta bursts speeds up  
633 movement initiation in healthy motor control : A double-blind sham- controlled study.  
634 *Journal of Neuroscience*. <https://doi.org/https://doi.org/10.1523/JNEUROSCI.0208-20.2020>

636 Herrmann, C. S., Strüber, D., Helfrich, R. F., & Engel, A. K. (2016). EEG oscillations: From  
637 correlation to causality. *International Journal of Psychophysiology*, 103, 12–21.  
638 <https://doi.org/10.1016/j.ijpsycho.2015.02.003>

639 Hsueh, J. J., Chen, T. S., Chen, J. J., & Shaw, F. Z. (2016). Neurofeedback training of EEG  
640 alpha rhythm enhances episodic and working memory. *Human Brain Mapping*, 37(7),  
641 2662–2675. <https://doi.org/10.1002/hbm.23201>

642 Jana, S., Hannah, R., Muralidharan, V., & Aron, A. R. (2020). Temporal cascade of frontal,  
643 motor and muscle processes underlying human action-stopping. *ELife*, 9, e50371.  
644 <https://doi.org/10.7554/elife.50371>

645 Jensen, O., & Mazaheri, A. (2010). Shaping functional architecture by oscillatory alpha  
646 activity: Gating by inhibition. *Frontiers in Human Neuroscience*, 4(Nov), 1–8.  
647 <https://doi.org/10.3389/fnhum.2010.00186>

648 Jeunet, C., Glize, B., McGonigal, A., Batail, J. M., & Micoulaud-Franchi, J. A. (2019). Using  
649 EEG-based brain computer interface and neurofeedback targeting sensorimotor  
650 rhythms to improve motor skills: Theoretical background, applications and prospects.  
651 *Neurophysiologie Clinique*, 49(2), 125–136. <https://doi.org/10.1016/j.neucli.2018.10.068>

652 Kasten, F. H., Duecker, K., Maack, M. C., Meiser, A., & Herrmann, C. S. (2019). Integrating  
653 electric field modeling and neuroimaging to explain inter-individual variability of tACS  
654 effects. *Nature Communications*, 10, 5427. <https://doi.org/10.1038/s41467-019-13417-6>

655 Kayser, J., & Tenke, C. E. (2006). Principal components analysis of Laplacian waveforms as  
656 a generic method for identifying ERP generator patterns: I. Evaluation with auditory  
657 oddball tasks. *Clinical Neurophysiology*, 117, 348–368.  
658 <https://doi.org/10.1016/j.clinph.2005.08.034>

659 Khanna, P., & Carmena, J. M. (2017). Beta band oscillations in motor cortex reflect neural

660 population signals that delay movement onset. *ELife*, 6, e24573.

661 <https://doi.org/10.7554/eLife.24573>

662 Lijffijt, M., Kenemans, J. L., Verbaten, M. N., & Van Engeland, H. (2005). A meta-analytic  
663 review of stopping performance in attention-deficit/ hyperactivity disorder: Deficient  
664 inhibitory motor control? *Journal of Abnormal Psychology*, 114(2), 216–222.  
665 <https://doi.org/10.1037/0021-843X.114.2.216>

666 Little, S., Bonaiuto, J., Barnes, G., & Bestmann, S. (2019). Human motor cortical beta bursts  
667 relate to movement planning and response errors. *PLoS Biology*, 17(10), e3000479.  
668 <https://doi.org/10.1371/journal.pbio.3000479>

669 Logan, G. D., & Cowan, W. B. (1984). On the ability to inhibit thought and action: A theory of  
670 an act of control. *Psychological Review*, 91(3), 295–327. <https://doi.org/10.1037/0033-295X.91.3.295>

672 Luijten, M., Littel, M., & Franken, I. H. A. (2011). Deficits in inhibitory control in smokers  
673 during a Go/Nogo task: An investigation using event-related brain potentials. *PLoS  
674 ONE*, 6(4), e18898. <https://doi.org/10.1371/journal.pone.0018898>

675 Marshall, L., Helgadóttir, H., Mölle, M., & Born, J. (2006). Boosting slow oscillations during  
676 sleep potentiates memory. *Nature*, 444, 610–613. <https://doi.org/10.1038/nature05278>

677 Micoulaud-Franchi, J. A., Geoffroy, P. A., Fond, G., Lopez, R., Bioulac, S., & Philip, P.  
678 (2014). EEG neurofeedback treatments in children with ADHD: An updated meta-  
679 analysis of randomized controlled trials. *Frontiers in Human Neuroscience*,  
680 8(November), 1–7. <https://doi.org/10.3389/fnhum.2014.00906>

681 Nolan, H., Whelan, R., & Reilly, R. B. (2010). FASTER: Fully Automated Statistical  
682 Thresholding for EEG artifact Rejection. *Journal of Neuroscience Methods*, 192(1),  
683 152–162. <https://doi.org/10.1016/j.jneumeth.2010.07.015>

684 Omejc, N., Rojc, B., Battaglini, P. P., & Marusic, U. (2019). Review of the therapeutic  
685 neurofeedback method using electroencephalography: EEG neurofeedback. *Bosnian  
686 Journal of Basic Medical Sciences*, 19(3), 213–220.  
687 <https://doi.org/10.17305/bjbm.2018.3785>

688 Polanía, R., Nitsche, M. A., & Ruff, C. C. (2018). Studying and modifying brain function with  
689 non-invasive brain stimulation. *Nature Neuroscience*, 21, 174–187.  
690 <https://doi.org/10.1038/s41593-017-0054-4>

691 R Core Team. (2020). R: A language and environment for statistical computing. *R: A*  
692 *Language and Environment for Statistical Computing. R Foundation for Statistical*  
693 *Computing, Vienna, Austria.*

694 Renard, Y., Lotte, F., Gibert, G., Congedo, M., Maby, E., Delannoy, V., et al. (2010).  
695 OpenViBE: An open-source software platform to design, test, and use brain-computer  
696 interfaces in real and virtual environments. *Presence: Teleoperators and Virtual*  
697 *Environments*. <https://doi.org/10.1162/pres.19.1.35>

698 Richards, J. B., Zhang, L., Mitchell, S. H., & de Wit, H. (1999). Delay or probability  
699 discounting in a model of impulsive behavior: effect of alcohol. *Journal of the*  
700 *Experimental Analysis of Behavior*, 71(2), 121–143.  
701 <https://doi.org/10.1901/jeab.1999.71-121>

702 Ros, T., Munneke, M. A. M., Ruge, D., Gruzelier, J. H., & Rothwell, J. C. (2010).  
703 Endogenous control of waking brain rhythms induces neuroplasticity in humans.  
704 *European Journal of Neuroscience*, 31(4), 770–778. <https://doi.org/10.1111/j.1460-9568.2010.07100.x>

706 Schaum, M., Pinzuti, E., Sebastian, A., Lieb, K., Fries, P., Mobsacher, A., et al. (2021). Right  
707 inferior frontal gyrus implements motor inhibitory control via beta-band oscillations in  
708 humans. *eLife*, 10, e61679. <https://doi.org/10.7554/eLife.61679>

709 Simon, C., Bolton, D. A. E., Kennedy, N. C., Soekadar, S. R., & Ruddy, K. L. (2021).  
710 Challenges and opportunities for the future of Brain-Computer Interface in  
711 neurorehabilitation. *Frontiers in Neuroscience*, 15(July).  
712 <https://doi.org/https://doi.org/10.3389/fnins.2021.699428>

713 Sitaram, R., Ros, T., Stoeckel, L., Haller, S., Scharnowski, F., Lewis-Peacock, J., et al.  
714 (2017). Closed-loop brain training: The science of neurofeedback. *Nature Reviews*  
715 *Neuroscience*, 18(2), 86–100. <https://doi.org/10.1038/nrn.2016.164>

716 Sonuga-Barke, E. J. S., Brandeis, D., Cortese, S., Daley, D., Ferrin, M., Holtmann, M., et al.  
717 (2013). Nonpharmacological Interventions for ADHD: Systematic Review and Meta-  
718 Analyses of Randomized Controlled Trials of Dietary and Psychological Treatments.  
719 *American Journal of Psychiatry*, 170, 275–289.  
720 <https://doi.org/https://doi.org/10.1176/appi.ajp.2012.12070991>

721 Sundby, K. K., Jana, S., & Aron, A. R. (2021). Double-blind disruption of right inferior frontal  
722 cortex with TMS reduces right frontal beta power for action stopping. *Journal of*  
723 *Neurophysiology*, 125(1), 140–153. <https://doi.org/10.1152/JN.00459.2020>

724 Swann, N., Tandon, N., Canolty, R., Ellmore, T. M., McEvoy, L. K., Dreyer, S., et al. (2009).  
725 Intracranial EEG Reveals a Time- and Frequency-Specific Role for the Right Inferior  
726 Frontal Gyrus and Primary Motor Cortex in Stopping Initiated Responses. *Journal of*  
727 *Neuroscience*, 29(40), 12675–12685. <https://doi.org/10.1523/JNEUROSCI.3359-09.2009>

728 Swann, N. C., Cai, W., Conner, C. R., Pieters, T. A., Claffey, M. P., George, J. S., et al.  
729 (2012). Roles for the pre-supplementary motor area and the right inferior frontal gyrus  
730 in stopping action: Electrophysiological responses and functional and structural  
731 connectivity. *NeuroImage*, 59(3), 2860–2870.  
732 <https://doi.org/10.1016/j.neuroimage.2011.09.049>

733 Thut, G., & Miniussi, C. (2009). New insights into rhythmic brain activity from TMS-EEG  
734 studies. *Trends in Cognitive Sciences*, 13(4), 182–189.  
735 <https://doi.org/10.1016/j.tics.2009.01.004>

736 Thut, G., Schyns, P. G., & Gross, J. (2011). Entrainment of perceptually relevant brain  
737 oscillations by non-invasive rhythmic stimulation of the human brain. *Frontiers in*  
738 *Psychology*, 2(July), 1–10. <https://doi.org/10.3389/fpsyg.2011.00170>

739 Verbruggen, F., Aron, A., Band, G., Beste, C., Bissett, P., Brockett, A. T., et al. (2019).  
740 Capturing the ability to inhibit actions and impulsive behaviors: A consensus guide to  
741 the stop-signal task. *ELife*, 8, e46323. <https://doi.org/10.31219/OSF.IO/8MZDU>

742 Vernon, D., Egner, T., Cooper, N., Compton, T., Neilands, C., Sheri, A., & Gruzelier, J.

744 (2003). The effect of training distinct neurofeedback protocols on aspects of cognitive  
745 performance. *International Journal of Psychophysiology*, 47(1), 75–85.  
746 [https://doi.org/10.1016/S0167-8760\(02\)00091-0](https://doi.org/10.1016/S0167-8760(02)00091-0)

747 Vosskuhl, J., Strüber, D., & Herrmann, C. S. (2018). Non-invasive Brain Stimulation: A  
748 Paradigm Shift in Understanding Brain Oscillations. *Frontiers in Human Neuroscience*,  
749 12(May), 1–19. <https://doi.org/10.3389/fnhum.2018.00211>

750 Wagner, J., Wessel, J. R., Ghahremani, A., & Aron, A. R. (2017). Establishing a Right  
751 Frontal Beta Signature for Stopping Action in Scalp EEG: Implications for Testing  
752 Inhibitory Control in Other Task Contexts. *Journal of Cognitive Neuroscience*, 30(1),  
753 107–118. <https://doi.org/10.1162/jocn>

754 Wessel, J. R. (2020).  $\beta$ -Bursts Reveal the Trial-to-Trial Dynamics of Movement Initiation and  
755 Cancellation. *The Journal of Neuroscience*, 40(2), 411–423.  
756 <https://doi.org/10.1523/JNEUROSCI.1887-19.2019>

757 Wessel, J. R., & Aron, A. R. (2017). On the Globality of Motor Suppression: Unexpected  
758 Events and Their Influence on Behavior and Cognition. *Neuron*, 93(2), 259–280.  
759 <https://doi.org/10.1016/j.neuron.2016.12.013>

760 Witte, M., Kober, S. E., Ninaus, M., Neuper, C., & Wood, G. (2013). Control beliefs can  
761 predict the ability to up-regulate sensorimotor rhythm during neurofeedback training.  
762 *Frontiers in Human Neuroscience*, 7(July), 1–8.  
763 <https://doi.org/10.3389/fnhum.2013.00478>

*bioRxiv versions accessed prior to 22-Nov-2021 contained a data error*